ELSEVIER

Pattern Recognition Letters 17 (1996) 1089–1099

Pattern Recognition Letters

Pose determination of a cylinder using reprojection transformation

Jen-Bin Huang [a], Zen Chen [a,*], Tsorng-Lin Chia [b]

[a] *Institute of Computer Science and Information Engineering, National Chiao Tung University, Hsinchu, Taiwan 30050*
[b] *Department of Electrical Engineering, Chung Cheng Institute of Technology, Taoyuan, Taiwan*

Received 12 June 1995; revised 29 May 1996

Abstract

Extracting useful and robust feature points from a cylinder image for 3D pose determination is a relatively difficult task, since there are no feature points or lines on the cylinder. In this study, a key vector from a cylinder image is found to yield a transformation. The cylinder is then "reprojected" from the original image to obtain a new image using the transformation. The new image reveals some important features capable of determining the 3D cylinder position robustly. The proposed method can yield an exact and analytical solution without the requirement of using any special marks, extra equipment or assumptions. Additionally, a problem in which both circles on the cylinder are not completely visible due to the viewing angle can be resolved by this method. Finally, experimental results are provided to verify the theory and show the robustness of our method.

Keywords: Pose determination; Reprojection transformation; 3D cylinder position

1. Introduction

Monocular computer vision is one of the challenging techniques for 3D scene analysis. Among the methodologies of monocular computer vision, perspective inversion is capable of determining 3D information for a desired object from its single perspective image based on the model knowledge. For industrial robots, tasks such as automatic manipulation are good applications in which a lot of object information is available. A cylinder is a primitive object of industrial products. There exist cylindrical objects, e.g., food cans, missiles, cylindrical containers, pipes, circular pillars, and wheels. Therefore, performing the pose determination of a cylinder is deemed necessary. In this study, an image transformation technique is used to develop a novel method capable of determining the 3D orientation and position of a right cylinder with known radius from a single image.

In the literature, approaches having used point/line correspondences or stereo vision (e.g., Liu et al., 1990 or Horaud et al., 1989) cannot be applied since there are no feature lines or points on a right cylinder. Also, extracting useful feature points from a right cylinder image is also relatively difficult under perspective projection. Some approaches having used the shape from shading (for instance, Woodham, 1978) could be employed to estimate the

* Corresponding author. E-mail: zchen@csie.nctu.edu.tw.

PII S0167-8655(96)00061-X

orientations of the cylindrical curved surface and the cylinder axis. However, these methods assumed that the illumination was simple and the surface reflectance was known. These assumptions are impractical (see Torras, 1992). Other investigators have labeled some special marks on the right cylinder to obtain extra constraints from their images. For instance, Lee et al. (1994) pasted a square label with known height on the cylinder to determine the pose parameters. Sai and Okawa (1993) marked the cylinder with four slits (two of them are parallel and the other two are angled) to solve this problem. These methods can simplify the mathematical deduction. However, in general there are no such special marks on the cylinder and their methods will be limited. The other investigators have used grid encoding techniques to determine the location and shape parameters (e.g., Chen et al., 1994; Wang, 1991) without a priori information of the object. However, extra lighting equipment is required. Shiu and Huang (1991) proposed a method using the endpoints of the projected line segments of the cylindrical curved surface (i.e., silhouette edges) to obtain simple equations for pose determination. However, the connection between the projected line segment and the projected circular curve is generally smooth. Thus, the exact connection points (i.e., ends of the projected lines) in the image are difficult to distinguish and extract; they are not robust features.

Some approaches (e.g., Safaee-Rad et al., 1990, 1992) could be used to estimate the 3D circle center and orientation from the projection of a circle on the cylinder by ellipse fitting first. However, the pose parameters of the lower partial circle image cannot be determined by those methods, since ellipse fitting generally becomes less accurate in such condition. Furthermore, as mentioned above, the exact connection points between the projected lines and projected curves are difficult to distinguish and extract; then the ellipse fitting becomes inaccurate. Besides, when the location of the camera center (i.e., the center of projection) is between the two circle planes of the cylinder, both circles on the cylinder are not completely visible (see Fig. 1). Consequently, the above methods based on circular features cannot be applied.

In this study, a novel approach is proposed to solve these problems encountered. First, we find a key vector from a cylinder image to yield a transformation. The transformation is then applied on the cylinder image to obtain a new image as if "reprojecting" the cylinder when the camera optical axis perpendicularly intersects the cylinder axis and the camera center remains fixed. As a result, some important features can be found to determine the pose parameters of the cylinder.

The merits of our method are summarized as follows.

(1) It provides an exact and analytical solution.

(2) In addition, our method does not require any extra marks or equipment. Therefore, it can be used in more extensive applications.

(3) Our method can clearly extract the key features on the symmetrical axis of the reprojected pattern. This scheme is helpful for the accurate pose determination. (The features used in Shiu and Huang's method (1991) are often ambiguous as mentioned above.)

(4) Our method is robust. A noise would generally cause a larger effect on the marks such as that used by Lee et al. (1994) and Sai and Okawa (1993) than on the longer line projections of the cylindrical curved surface used in our method, since a mark on a cylinder is always smaller than the cylinder itself.

(5) Besides, our method can solve the problem in which both circles on the cylinder are not completely visible due to the viewing angle.

2. Problem formulation

Fig. 1 illustrates the perspective projection geometry of a cylinder. Under the assumption that the

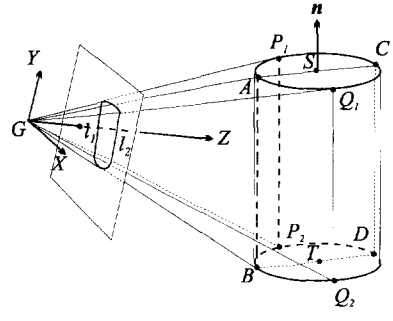

Fig. 1. The projection of a cylinder.

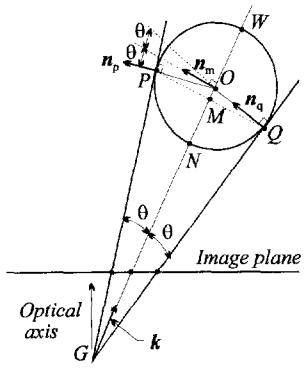

Fig. 2. The top view of the cylinder projection.

camera center is above the upper circle plane or below the lower circle plane, a projection of a complete circle would exist. On the other hand, a complete circle cannot be observed if the camera center is between the two circle planes on the cylinder (see Fig. 1). Our approach can solve both of these cases since it does not need a completely visible circle. In order to ensure an image is the projection of a cylinder, the cylindrical curved surface is assumed here to be visible in the image. From the image, the 3D positions of the upper and lower circle centers can be estimated as well as the direction of the cylinder axis with respect to the viewing (camera) coordinate system.

Let the horizontal axis of the image plane be the x axis and the vertical axis be the y axis. The viewing (camera) coordinate system consists of the X, Y and Z axes. The X and Y axes are parallel to the x and y axes. The Z axis coincides with the camera optical axis. Point G is the camera center. As shown in Fig. 1, vector $\boldsymbol{n}$ is the orientation of the cylinder axis. Planes GP_1P_2 and GQ_1Q_2 are tangent to the cylinder. Points S and T are the upper and lower circle centers. Lines l_1 and l_2 are the projections of lines $\overline{P_1P_2}$ and $\overline{Q_1Q_2}$. Fig. 2 shows the top view of Fig. 1. Points P, Q, N, W and O are the orthographic projections of the lines $\overline{P_1P_2}$, $\overline{Q_1Q_2}$, $\overline{AB}$, $\overline{CD}$ and the cylinder axis, respectively. Also, allow vectors $\boldsymbol{n}_p$ and $\boldsymbol{n}_q$ to be the surface normals of the planes GP_1P_2 and GQ_1Q_2, respectively.

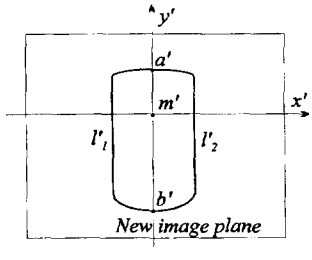

Fig. 3. The canonical image of a cylinder.

3. Finding key vector for reprojection transformation

We shall estimate a transformation (that is, the reprojection transformation) and then perform the transformation on the cylinder image to obtain a new image (the canonical image, see Fig. 3) and the key features for pose determination later. First, a key vector has to be found to solve the reprojection transformation. Let the equation of line l_1 be $a_p x + b_p y + c_p = 0$ in the image coordinate system. The parameters a_p, b_p and c_p can be obtained from the image plane. Line l_1 and the camera center G define the plane GP_1P_2. Since the equation of the image plane is $Z = f$, where f is the effective focal length, the equation of the plane GP_1P_2 is $a_pX + b_pY + c_p/fZ = 0$ in the viewing coordinate system. Thus, the normal vector $\boldsymbol{n}_p$ of the plane GP_1P_2 is $(a_p, b_p, c_p/f)$.

In the same manner, we can obtain the normal vector $\boldsymbol{n}_q$ of the plane GQ_1Q_2. Once the vectors $\boldsymbol{n}_p$ and $\boldsymbol{n}_q$ are obtained, the direction of the cylinder axis in the viewing coordinate system is

$$\boldsymbol{n} = \boldsymbol{n}_p \times \boldsymbol{n}_q.$$

Let the plane GST, passing through both the cylinder axis and point G, bisect the cylinder at the four corner points A, B, C and D. Since the plane GST is the bisector of the planes GP_1P_2 and GQ_1Q_2, the normal vector $\boldsymbol{n}_m$ of the plane GST is given by

$$\boldsymbol{n}_m = \boldsymbol{n}_p + \boldsymbol{n}_q.$$

Let θ be the angle between $\boldsymbol{n}_m$ and $\boldsymbol{n}_p$ (or $\boldsymbol{n}_q$). Since the plane GST is the bisector of the planes GP_1P_2 and GQ_1Q_2, both $\angle PGO$ and $\angle QGO$ are equal to θ. Also, let $\boldsymbol{k}$ be a vector (similar to $\overrightarrow{GO}$) which perpendicularly intersects the cylinder axis. After the direction of the cylinder axis and the

surface normal of the plane GST are obtained, vector $\boldsymbol{k}$ can be calculated which perpendicularly intersects the cylinder axis as follows:

$$\boldsymbol{k} = (\boldsymbol{n}_m \times \boldsymbol{n}) / \| \boldsymbol{n}_m \times \boldsymbol{n} \|.$$

Vector $\boldsymbol{k}$ is used in the next section to solve the reprojection transformation. After the reprojection transformation, the camera optical axis is realigned to vector $\boldsymbol{k}$.

4. Obtaining the canonical image by reprojection transformation

As mentioned above, extracting useful or robust features from a cylinder image is relatively difficult. In our approach, based on vector $\boldsymbol{k}$, a transformation is applied on the original cylinder image to obtain a new image as if the new cylinder image is taken when the camera optical axis perpendicularly intersects the cylinder axis, and the cylinder axis is on the new $Y'Z'$ plane (Fig. 4 presents the preliminary concept and Fig. 5 is the reprojection geometry). This transformation is referred to as *reprojection transformation* and the new image is referred to as *canonical image*. The objective includes locating useful and robust features as well as simplifying the mathematical deduction to perform pose determination from the canonical image. The following scheme illustrates the procedure.

First, we construct a new camera ($X'Y'Z'$) coordinate system such that the new optical axis (the new Z' axis) coincides with the vector $\boldsymbol{k}$ and the $Y'Z'$ plane with the plane GST (thus the cylinder axis is parallel to the Y' axis). The new image ($x'y'$) plane is at $Z' = f$ and the x' and y' axes are parallel to the X' and Y' axes. Let $\boldsymbol{i}$, $\boldsymbol{j}$ and $\boldsymbol{k}$ be the unit vectors in X', Y' and Z' direction with respect to the original camera coordinate system, respectively. Also let $M = (X_M, Y_M, Z_M)$ be a point in the original camera coordinate system and its image be (x, y). A rotation $\boldsymbol{R}$ can be made to transform point M to (X'_M, Y'_M, Z'_M) in the new $X'Y'Z'$ coordinate system by $(X'_M, Y'_M, Z'_M)^{\mathrm{T}} = \boldsymbol{R}(X_M, Y_M, Z_M)^{\mathrm{T}}$, where $\boldsymbol{R} = (\boldsymbol{i} \mid \boldsymbol{j} \mid \boldsymbol{k})^{\mathrm{T}}$ and "|" denotes the matrix partitioning. Point M is then reprojected to point (x', y') on the new image plane, where $x' = fX'/Z'$ and $y' = fY'/Z'$. Thus for a point (x, y) on the original image plane, the new image coordinates after the reprojection can be expressed as follows:

$$x' = f\frac{(X_M, Y_M, Z_M)^{\mathrm{T}} \cdot \boldsymbol{i}}{(X_M, Y_M, Z_M)^{\mathrm{T}} \cdot \boldsymbol{k}} = f\frac{(x, y, f)^{\mathrm{T}} \cdot \boldsymbol{i}}{(x, y, f)^{\mathrm{T}} \cdot \boldsymbol{k}}$$

and

$$y' = f\frac{(X_M, Y_M, Z_M)^{\mathrm{T}} \cdot \boldsymbol{j}}{(X_M, Y_M, Z_M)^{\mathrm{T}} \cdot \boldsymbol{k}} = f\frac{(x, y, f)^{\mathrm{T}} \cdot \boldsymbol{j}}{(x, y, f)^{\mathrm{T}} \cdot \boldsymbol{k}}.$$

Therefore, we can obtain the new image of point M in the new $x'y'$ image plane as long as the original image point M is known. After applying the reprojection transformation to the original cylinder image, we can subsequently obtain a new image (the canonical image). In the $X'Y'Z'$ coordinate system, the camera optical axis intersects the cylinder axis perpendicularly. The cylinder axis is parallel to the image plane. Thus the new image obtained is a symmetrical pattern with respect to the y' axis (see Fig. 3) since the $Y'Z'$ plane (i.e., the plane GST)

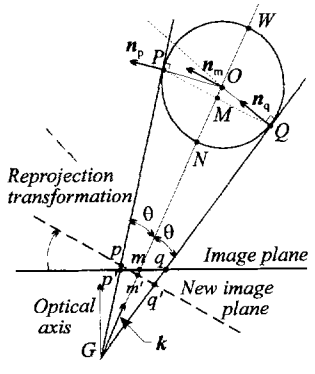

Fig. 4. The preliminary concept of the reprojection transformation.

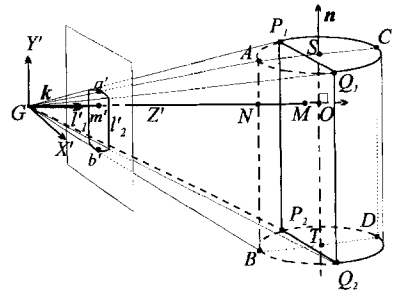

Fig. 5. Reprojection geometry.

cuts the cylinder into two symmetrical halves. Furthermore, the new image lines l'_1 and l'_2 of the lines $\overline{P_1P_2}$ and $\overline{Q_1Q_2}$ are parallel to each other and parallel to the y' axis, too.

In Fig. 3, points a' and b' (i.e., the projections of points A and B) appear on the y' axis. If the camera center is not between the two cylinder circle planes, the projected points c' (or d') of points C (or D) would also be on the y' axis. These special geometrical properties contain useful and important information for the pose determination of the cylinder. In the following section, the contour points on the y' axis are used as the *key features* to obtain the pose parameters.

5. Solving the pose parameters from the canonical image

Fig. 6 illustrates the side view of the reprojection of a cylinder (that is on the $Y'Z'$ plane) for the canonical image. In the situation in which the camera center is not between the upper and lower circle planes, the camera optical axis does not intersect the cylinder under a canonical image (since the new camera optical axis perpendicularly intersects the cylinder axis). Without loss of generality, an extension cylinder of infinite length is constructed here and points N and W are allowed to be the intersection points between the extension cylindrical curved surface and the camera optical axis. Let point M be the intersection point between the optical axis and the plane $P_1P_2Q_1Q_2$. Point m is the corresponding image of point M. Point O is the intersection point between the new camera optical axis and the cylinder axis. Let R_c be the cylinder radius. The pose

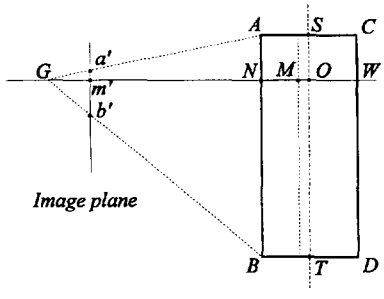

Fig. 6. The side view for a canonical image.

determination of a cylinder can be deduced from the canonical image as follows.

From Fig. 4, θ is given by

$$\theta = \tan^{-1}\left(|\overline{pm'}|/f\right) \quad \text{and} \quad |\overline{PM}| = R_c \cos\theta.$$

By the similarity of the triangles $\triangle GPM$ and $\triangle Gpm$,

$$|\overline{PM}|/|\overline{pm'}| = |\overline{GM}|/f$$

and then

$$\overrightarrow{GM} = \left(0, 0, f|\overline{PM}|/|\overline{pm'}|\right)^{\mathrm{T}}.$$

Thus, $\overrightarrow{GM}$ can be calculated from the canonical image in the $X'Y'Z'$ coordinate system. In addition, in Fig. 6

$$\overrightarrow{MN} = \left(0, 0, -(R_c - R_c \sin\theta)\right)^{\mathrm{T}}$$

and

$$\overrightarrow{MW} = \left(0, 0, (R_c + R_c \sin\theta)\right)^{\mathrm{T}}.$$

Let y_a, y_b and y_c represent the y' coordinates of the points a', b' and c'. (If a complete circle is visible, we assume that point C is visible in the following. On the other hand, if point D is visible, its image point d' can be used to solve the pose parameter in a similar way). From Fig. 6, we have

$$\overrightarrow{GN} = \overrightarrow{GM} + \overrightarrow{MN} \quad \text{and} \quad \overrightarrow{GW} = \overrightarrow{GM} + \overrightarrow{MW}.$$

$\overrightarrow{NA}$, $\overrightarrow{NB}$ and $\overrightarrow{WC}$ then can be expressed as

$$\overrightarrow{NA} = \left(0, s|\overline{NA}|, 0\right)^{\mathrm{T}} \quad \text{where } s = 1 \text{ if } y_a \geqslant 0, \; s = -1 \text{ otherwise;}$$

$$\overrightarrow{NB} = \left(0, s|\overline{NB}|, 0\right)^{\mathrm{T}} \quad \text{where } s = 1 \text{ if } y_b \geqslant 0, \; s = -1 \text{ otherwise;}$$

$$\overrightarrow{WC} = \left(0, s|\overline{WC}|, 0\right)^{\mathrm{T}} \quad \text{where } s = 1 \text{ if } y_c \geqslant 0, \; s = -1 \text{ otherwise.}$$

Since $\overrightarrow{GM}$, $\overrightarrow{MN}$ and $\overrightarrow{MW}$ are readily known, $\overrightarrow{GN}$ and $\overrightarrow{GW}$ can be yielded. Furthermore, based on the similarity of the triangles $\triangle GNA$ and $\triangle Gm'd'$ (or of $\triangle GWC$ and $\triangle Gm'c'$) as well as of $\triangle GNB$ and $\triangle Gm'b'$, the following equations are used to solve $\overrightarrow{NA}$ (or $\overrightarrow{WC}$) and $\overrightarrow{NB}$:

$$|\overline{NA}| = |\overline{GN}|\,|\overline{m'd'}|/f \quad \left(\text{or } |\overline{WC}| = |\overline{GW}|\,|\overline{m'c'}|/f\right)$$

and

$$|\overline{NB}| = |\overline{GN}|\,|\overline{m'b'}|/f.$$

Once $\overrightarrow{NA}$ (or $\overrightarrow{WC}$) and NB are available, $\overrightarrow{GA}$ (or $\overrightarrow{GC}$) and $\overrightarrow{GB}$ can be obtained as follows:

$$\overrightarrow{GA} = \overrightarrow{GN} + \overrightarrow{NA} \quad (\text{or } \overrightarrow{GC} = \overrightarrow{GW} + \overrightarrow{WC})$$

and

$$\overrightarrow{GB} = \overrightarrow{GN} + \overrightarrow{NB}.$$

Therefore, the two circle centers (position vectors) on the cylinder can be obtained by

$$\overrightarrow{GS} = \overrightarrow{GA} + (0, 0, R_c)^{\mathrm{T}}$$

$$\left(\text{or } \overrightarrow{GS} = \overrightarrow{GI} - (0, 0, R_c)^{\mathrm{T}}\right),$$

and

$$\overrightarrow{GT} = \overrightarrow{GB} + (0, 0, R_c)^{\mathrm{T}},$$

and the height of the cylinder H is

$$H = |\overrightarrow{GT} - \overrightarrow{GS}| \text{ or } |\overrightarrow{GB} - \overrightarrow{GA}|.$$

6. Pose determination via inverse transformation

Let $\overrightarrow{GS}^*$ and $\overrightarrow{GT}^*$ be the vectors of the cylinder's upper and lower circle centers in the original coordinate system. The difference between the canonical image and the original image is only the rotation $\boldsymbol{R}$ (in the reprojection transformation). The transformation matrix and the vectors of the circle centers in the canonical image have been mentioned above. Therefore, the position vectors of the two circle centers on the cylinder in the original coordinate system can be obtained by inverse transformation as follows:

$$\overrightarrow{GS} = \boldsymbol{R}^{\mathrm{T}}\overrightarrow{GS} \quad \text{and} \quad \overrightarrow{GT}^* = \boldsymbol{R}^{\mathrm{T}}\overrightarrow{GT}.$$

Finally, the 3D position (including the two circle centers) and the orientation of the cylinder have so far been solved.

7. Experiment results

In this section, we evaluate the performance of our method. In the first experiment, different cylinders are used to verify whether our method can effectively determine the pose parameters. Also, both cases with/without the projection of a complete circle due to the viewing angle are examined. Here the accuracy of our method is reported on the cylinder height. In the second experiment, experimental comparisons between our method and Safaee-Rad's method are given. In the third experiment, the noise sensitivity is examined by adding random noise with a Gaussian distribution to the cylinder image.

In the experiments, an ELMO SE320 CCD camera is used to capture the images. The intrinsic parameters of the camera have been calibrated. An NTSC signal output from the camera is digitized into an array of 512×480 pixels by a VFG-512 digitizer card. Moreover, the digitizer is added on a 486 PC which executes our program in C language. The cylinders are then put on a homogeneous background. The pose determination procedure is summarized as follows.

Step 1. Fit the line equations of the projected lines l_1 and l_2 in the cylinder image. A line fitting algorithm (Haralick and Shapiro, 1992) is used to obtain the equations of lines l_1 and l_2.

Step 2. Calculate the key vector $\boldsymbol{k}$ for estimating the reprojection transformation. The normal vectors $\boldsymbol{n}_p$, $\boldsymbol{n}_q$ and $\boldsymbol{n}_m$ of the planes GP_1P_2, GQ_1Q_2, GST, and the direction vector $\boldsymbol{n}$ of the cylinder axis are calculated by vector operations. As a result, the vector $\boldsymbol{k}$ can be found by a vector cross product (i.e. $\boldsymbol{k} = \boldsymbol{n}_m \times \boldsymbol{n}$) to perpendicularly intersect the cylinder axis.

Step 3. Obtain the reprojection transformation matrix and then the canonical image. Once key vector $\boldsymbol{k}$ is obtained, directly use the formulas in Section 4 to determine the transformation matrix for the reprojection transformation. Then apply the reprojection transformation to obtain the new canonical cylinder image.

Step 4. Extract the key features to determine the pose parameters in the canonical image. The key features are located on the y' axis. Find the point right on the y' axis (or the plane GST) from the projected curves. (Here interpolation between points on the reprojected curves is used to find the key features.) Thus, the pose parameters $\overrightarrow{GS}$ and $\overrightarrow{GT}$ of the cylinder in the canonical image can be determined by vector operations as mentioned in Section 5.

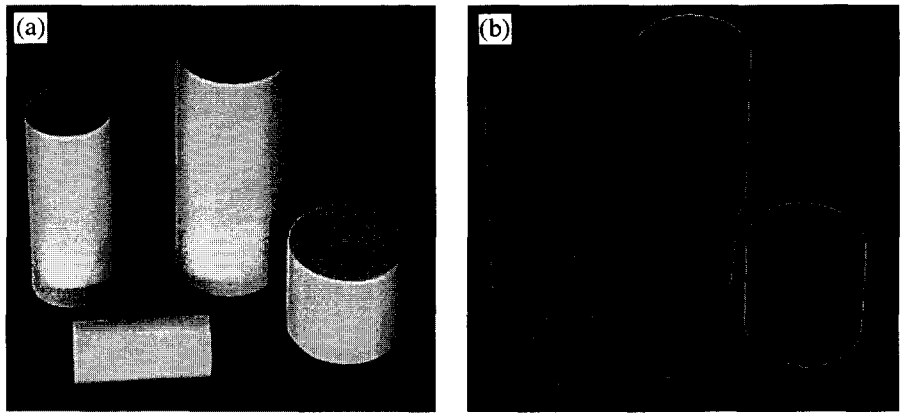

Fig. 7. Cylinder height estimation in Experiment 1. (a) Original image. (b) Contours extracted.

Step 5. Pose determination of the cylinder via inverse transformation. Transforming the vectors $\overrightarrow{GS}$ and $\overrightarrow{GT}$ obtained in Step 4 back to the original coordinate system by $\boldsymbol{R}^{\mathrm{T}}$, we can obtain the positions of both circle centers on the cylinder.

7.1. Experiment 1

In this test, an image with four cylinders (as shown in Fig. 7) with/without the projection of a complete circle is dealt with. Also, the height parameter of a cylinder is estimated. The cylinder images are taken under the assumption that the radius of each cylinder is known. We estimate the positions of the two cylinder circle centers and the orientations of the cylinder axis from the image, then the cylinder height. The accuracy is reported on the error of the height as indicated in Table 1. The height error rate is around 3%. The results indicate that our method functions well with cylinders of different size and operates properly no matter whether a complete circle is visible.

7.2. Experiment 2

In this test, cylinder 1 (with a height of 124.8 mm) is placed on a rotating table. Different rotation angles are selected to capture some images as shown in Figs. 8(a)–(d), so that the angles from Fig. 8(a) to Figs. 8(b), (c) and (d) are 50, −100, −40 degrees, respectively, and the distances for the upper circle center from Fig. 8(a) to Figs. 8(b), (c) and (d) are 105.5, 191.2 and 85.4 mm, respectively. The visible circle center is kept unchanged. The 3D pose parameters of the cylinder are then estimated for each image by both Safaee-Rad's method and our method. In our method, a threshold value is used to segment the cylinder image then contour following is applied to obtain the contour as depicted in Figs. 8(e)–(h). In the implementation of Safaee-Rad's method, we use

Table 1
The estimated position, orientation and height of cylinders in Experiment 1

Cylinder number	Height (mm)	Upper circle center	Lower circle center	Estimated height (mm)	Error (%)
1	124.8	(6.33, −69.38, 1061.27)	(4.83, 35.00, 1135.89)	128.32	2.82
2	100.6	(−89.72, −38.87, 1041.49)	(−92.02, 44.39, 1102.43)	103.21	2.59
3	49.2	(74.03, 22.71, 1056.25)	(74.02, 63.99, 1087.39)	51.70	5.09
4	79.3	(−84.34, 75.46, 1006.99)	(−7.51, 73.26, 1020.29)	78.00	1.63

Note: The diameters (in mm) of circles 1, 2, 3 and 4 are 69.0, 50.5, 70.5 and 29.5, respectively.

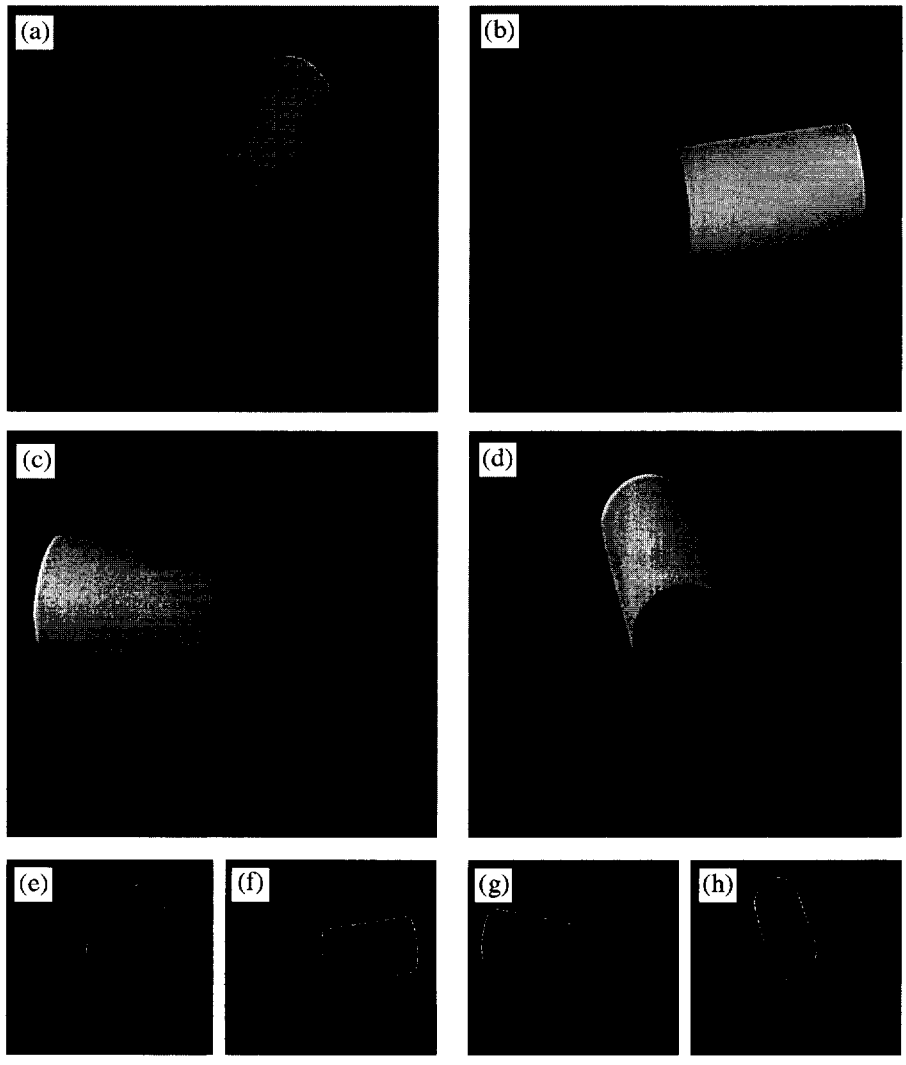

Fig. 8. Rotation and translation estimation in Experiment 2. (a), (e) Original configuration and its contour. (b), (f) Rotated 50 degs. and translated 105.5 mm. (c), (g) Rotated −100 degs. and translated 191.2 mm. (d), (h) Rotated −40 degs. and translated 85.4 mm.

the Laplacian operator then contour following to obtain the elliptic curve contour for ellipse fitting.

After pose determination, a verification is made as to whether the estimated rotation angle and the translational distance (between two images) are equal to the specified values. (In Safaee-Rad's method, both the top circle (i.e., the partially visible circle) contour and the base circle (i.e., the completely visible circle) contour can be used to estimate the 3D cylinder axis orientation. Here the base circle yields a better axis orientation.) The accuracy is reported on the errors of the translational distances, rotation angles, and the cylinder height. These results are summarized in Tables 2 and 3. The rotation angles and the location of the base circle center are almost the same for both Safaee-Rad's method and our method. However, the translational distance derived from the location of the partially visible circle has a large difference between these two methods. The distance error rate (translational distance error/reference distance * 100%) for the top circle center is below 2.0% for our method while up to 31.3% for Safaee-

Table 2
The estimated position, orientation and height of cylinders in Experiment 2

Rotation angle / Translation distance		Two cylinder circle center		Cylinder axis vector	
		Our method	Safaee-Rad's method	Our method	Safaee-Rad's method
−50 deg	Top circle	(118.40, −4.79, 1288.17)	(138.78, −6.19, 1446.42)	(0.963, −0.123, 0.241)	(0.972, −0.130, 0.194)
	Base circle	(−1.59, 10.52, 1258.08)	(−3.00, 11.06, 1286.06)		
105.5 mm	Distance/Angle (error)	107.48 mm (1.89%)	11.92 mm (11.29%)	48.46 deg (1.54 deg)	50.11 deg (0.11 deg)
100 deg	Top circle	(−119.93, −14.31, 1291.50)	(−145.95, −17.35, 1486.97)	(−0.939, −0.173, 0.299)	(−0.952, −0.179, 0.249)
	Base circle	(−3.97, 7.01, 1254.60)	(−2.83, 8.05, 1248.47)		
191.2 mm	Distance/Angle (error)	192.09 mm (0.47%)	27.62 mm (14.45%)	95.74 deg (4.26 deg)	98.56 deg (1.44 deg)
40 deg	Top circle	(−28.42, −58.24, 1349.76)	(−29.61, −60.67, 1370.84)	(−0.211, −0.553, 0.806)	(−0.225, −0.561, 0.797)
	Base circle	(−2.43, 9.87, 1250.38)	(−2.49, 10.23, 1253.23)		
85.4 mm	Distance/Angle (error)	84.47 mm (1.05%)	26.75 mm (31.33%)	38.13 deg (1.87 deg)	39.39 deg (0.61 deg)

Original circle center: (55.12, 52.40, 1360.83) and surface normal: (0.437, −0.482, 0.759)

Table 3
The cylinder height estimation in Experiment 2

Method	Image (a) Height (error)	Image (b) Height (error)	Image (c) Height (error)	Image (d) Height (error)
Our method	130.28 mm (4.39%)	124.65 mm (0.12%)	123.55 mm (1.00%)	123.25 mm (1.24%)
Safaee-Rad's method	199.90 mm (60.18%)	214.74 mm (72.07%)	279.30 mm (123.80%)	139.98 mm (12.16%)

Reference cylinder height = 124.8 mm.

Rad's method. Furthermore, the cylinder height error rate (height error/cylinder height * 100%) is below 5.0% in our method and up to 139.9% in Safaee-Rad's method.

These results in Tables 2 and 3 illustrate that if the entire circular surface of the cylinder is visible and if the ellipse fitting is accurate, both methods functions equally well. However, in the case of partial elliptic contour fitting, the length of the partial ellipse in a cylinder image is generally less than one half of the ellipse and two ends of the major axis are not fully available. The ellipse fitting becomes imprecise and unreliable. So the translational distance and cylinder height estimated by Safaee-Rad's method have larger errors. Furthermore, the connection between the partial ellipse and the lateral (silhouette) edges in the cylinder image is generally smooth, thus, the connection point is difficult to extract (even impossible by human eyes usually). This leads to an additional error. Thus, Safaee-Rad's method is less accurate in the partially visible circle of a cylinder. In addition, if both circles on the cylinder are not completely visible, Safaee-Rad's method cannot be applied.

7.3. Experiment 3

To test the robustness of our method against noise, the x and y coordinates of the contour points in Fig. 8(c) are added with random noise which is a Gaussian distribution with zero mean and standard deviation (sd) of 1, 2 and 3 pixels, respectively. Cylinder pose determination is then performed to obtain the circle centers of the cylinder and the cylinder height. We repeat this test 1000 times. The sensitivity is estimated by the mean deviation (MD) and the standard deviation (SD) (defined as follows) of the cylinder height and position. Those results are summarized in Table 4. The symbols dX, dY and dZ represent the errors in the X, Y and Z coordinates, and dS represents the mean distance error. Also, dH is the error of the cylinder height. The mean deviation of the position ranges from 1.90 to 5.91 mm and the range of the cylinder height mean deviation is between 0.94 and 2.86 mm. The results demonstrate that the noise effect is slight in our method even in a noisy condition with $sd = 3$ pixels.

$$MD = \frac{1}{n}\sum_{i=1}^{n} | x_i - \bar{x} |$$

and

$$SD = \sqrt{\frac{1}{n-1}\sum_{i=1}^{n} (x_i - \bar{x})^2},$$

where $\bar{x}$ is the value (position or height) without noise.

Table 4
The statistical errors for the sensitivity analysis (1000 samples)

Noise level	dX (mm)		dY (mm)		dZ (mm)		dS (mm)	dH (mm)
	MD	SD	MD	SD	MD	SD	MD	MD
$sd = 1$	0.78	0.99	0.16	0.21	1.58	2.01	1.90	0.94
$sd = 2$	1.65	2.05	0.34	0.42	3.24	4.02	3.90	1.95
$sd = 3$	2.40	3.03	0.50	0.63	4.97	6.21	5.91	2.86

8. Conclusion

In this study, we propose a new approach for 3D pose determination of a cylinder from a single image. From the cylinder image, a key vector is found to yield the reprojection transformation. The transformation is then applied on the cylinder image to obtain the canonical image. As a result, the key features can be exposed and extracted clearly. In addition, the mathematical deduction can be simplified to determine the pose parameters of the cylinder by vector operations. Our approach can obtain an exact analytical solution without the constraints of labeling feature marks on the cylinder or applying ellipse fitting which is less accurate in the partially visible circle of a cylinder. The proposed scheme also functions well under the circumstance in which the circles on the cylinder are not completely visible as shown in Fig. 1. Thus wider applications can hopefully be made than in traditional approaches. After the reprojection transformation, the key features can be clearly located and extracted. This scheme is helpful for accurate pose determination. Furthermore, since a special mark labeled on a cylinder is always smaller than the cylinder itself, noise would cause a larger effect on the marks. Thus, our method would also be more robust.

The experimental results indicate that the error rate of our method is mostly below 5%. Besides, the direction of the cylinder axis can be estimated well. Furthermore, even in a noisy environment ($sd = 3$ pixels), our method still operates properly. The results obtained here confirm the validity of our theory. In the near future, we plan to extend this approach to solve the pose determination of other objects such as circles, cones and spheres.

References

Chen, Z., T.-L. Chia and S.-Y. Ho (1994). Measuring 3-D location and shape parameters of cylinders by a spatial encoding technique. *IEEE Trans. Robot. Automat.* 10, 632–647.

Haralick, R.M. and L.G. Shapiro (1992). *Computer and Robot Vision.* Addison-Wesley, New York.

Horaud, R., B. Conio and O. Leboulleux (1989). An analytic solution for the perspective 4-point problem. *Comput. Vision Graphics Image Process.* 47, 33–44.

Lee, J.-D., J.-Y. Lee, Y.-C. You and C.-H. Chen (1994). Determining location and orientation of a labeled cylinder using point-pair estimation algorithm. *Internat. J. Pattern Recognition Artificial Intelligence* 8, 351–370.

Liu,Y. T.S. Huang and O.D. Faugeras (1990). Determination of camera location from 2-D to 3-D line and point correspondences. *IEEE Trans. Pattern Anal. Mach. Intell.* 12 (1), 28–37.

Safaee-Rad, R., K.C. Smith and B. Benhabib (1990). Accurate estimation of elliptical shape parameters from a grey-level image. *IEEE 10th Internat. Conf. on Pattern Recognition,* Atlantic City, NJ, Vol. II, 20–26.

Safaee-Rad, R., I. Tchoukanov, K.C. Smith and B. Benhabib (1992). Three-dimension of circular features for machine vision. *IEEE Trans. Robot. Automat.* 8, 624–640.

Sai, H. and Y. Okawa (1993). A structured sign for guiding movable robots. *Advanced Robotics* 7, 235–249.

Shiu, Y.C. and C. Huang (1991). Pose determination of circular cylinders using elliptical and side projection. *Proc. IEEE,* 265–268.

Torras, C. (1992). *Computer Vision: Theory and Industrial Application.* Springer, New York.

Wang, Y.F. (1991). Characterizing 3D surface structured from visual images. *IEEE Trans. Pattern Anal. Mach. Intell.* 13, 51–60.

Woodham, R.J. (1978). Photometric stereo: a reflectance map technique for determining surface orientation from image intensity. *Proc. 22nd Internat. Symp. Society of Photo-optical Instrumentation Engineers,* San Diego, CA, 136–143.